Article

Magnussonite, $Mn^{2+}_{18} (As^{3+}O_3)_6 Mn^{1+}_x(H_2O, Cl_x, \square)$: Re-Examination of the Structure and the $[Mn^{1+}(As^{3+}O_3)_6]$ Cluster

Frank C. Hawthorne [1],*, John M. Hughes [2] and Chi Ma [3]

1   Department of Geological Sciences, University of Manitoba, Winnipeg, MB R3T 2N2, Canada
2   Department of Geology, University of Vermont, Burlington, VT 05405, USA
3   Division of Geological and Planetary Sciences, California Institute of Technology, Pasadena, CA 91125, USA
*   Correspondence: frank.hawthorne@umanitoba.ca

Abstract: The crystal structure of magnussonite, ideally $Mn^{2+}_{18}[As^{3+}_6(Mn^{1+}_x)O_{18}]_2[(H_2O, Cl_x, \square) (H_2O, \square)]_2$, from Långban, Sweden, was refined to an R_1-index of 1.19% and the structure proposed by Moore and Araki (1979) is confirmed. Magnussonite has a densely packed structure of $(Mn\varphi_n)$ polyhedra, $\varphi = (O^{2-}, H_2O, Cl^-)$, and $(As^{3+}O_3)$ triangular pyramids that is best envisaged as layers of polyhedra in the same way as many of the other manganese-arsenite-arsenate structures from Långban. There are two distinct layers in magnussonite; the two layers may be combined into a slab that stacks along the a-direction with rotations between adjacent slabs. A surprising feature of the dense-packed magnussonite atomic arrangement is an array of structural channels along [111] that contain much of the disorder that occurs in the magnussonite structure. The channels contain the partly occupied MX site on the central axis of the channel, and the CLW2 site (with extremely low occupancy), also on the central axis of the channel. The CLW2 site, previously unrecognized in the magnussonite structure, contains H_2O, whereas the minor Cl in the structure resides in the CLW1 channel site, balancing the charge of the MX-site occupant. The MX site on the central axis of the channels displays a coordination known only in Långban minerals. In the local arrangement around the unoccupied MX site, the neighboring $(As^{3+}O_3)$ groups project their associated stereoactive lone-pairs of electrons into the channel. Where the MX site is occupied by Mn, there are six lone-pairs of electrons pointing toward Mn; the 18-electron rule predicts/rationalizes formulae for this stable transition-metal cluster. The $(As^{3+}O_3)$ groups and MX occupant form a $[Mn^+(As^{3+}O_3)_6]$ arrangement in accord with the 18-electron rule where Mn^+ contributes 6 3d electrons and the six lone-pairs of the $[(As^{3+}O_3)_6]$ arrangement contribute 12 electrons for a total of 18 electrons that form nine molecular orbitals that are metal-ligand bonds or non-bonding. Magnussonite and dixenite, another basic manganese-iron arsenate-arsenite-silicate mineral of the Långban-type deposits in Bergslagen, Sweden, are the only two minerals known with such local $[M^+(As^{3+}O_3)_n]$ transition-metal clusters. The presence of these exotic clusters in structures containing densely packed Mn^{2+} octahedra is not understood at present.

Keywords: magnussonite; crystal structure; metallic clusters; Långban; Sweden

1. Introduction

During comprehensive study of the minerals of Långban, Sweden, Paul B. Moore and Takaharu Araki unraveled the atomic arrangements of dixenite, ideally $Cu^+Fe^{3+}Mn^{2+}_{14}(As^{5+}O_4)(As^{3+}O_3)_5(SiO_4)_2(OH)_6$ [1], and magnussonite, putatively $Mn^{2+}_{18}[As^{3+}_6(Mn^{1+})O_{18}]_2Cl_2$ [2]. The solutions were both a *tour de force* for the equipment and software of the time, but lingering details caused Paul Moore to urge us to re-examine the structures to provide more detail, particularly with regard to the metal clusters contained in both structures. Dixenite contains clusters of $[Cu^+(As^{3+}O_3)_4]$ in which Cu^+ bonds to four As^{3+} ions in a metal cluster, and magnussonite contains Mn^{1+} bonded to six As^{3+} ions

in a $[Mn^+(As^{3+}O_3)_6]$ metal cluster. As far as we are aware, these are the only examples of such metallic clusters in minerals or synthetic inorganic crystals and are of interest in the broader context of bonding in inorganic crystal structures.

Both these minerals occur in the (Fe-Mn)-oxide ore deposits at Långban, Sweden [3–8], and we have a long-term interest in the basic Mn-arsenate-silicate minerals from this locality [9–12]. In [13], the details of the atomic arrangement of dixenite were described, and four of the five distinct layers in the repeat unit of the cell were related to the layers in mcgovernite [9]. It was also shown how the central Cu^+ ion in the metallic cluster occupies the positions normally taken by the stereoactive lone-pairs of electrons that generally characterize As^{3+} in triangular-pyramidal coordination by O; the stereoactive lone-pair behavior that is characteristic of $(As^{3+}O_3)$ trigonal pyramids is suppressed by the coordination of Cu^+ by four As^{3+} ions.

In this work we continue our examination of metallic clusters in minerals in a re-examination of the atomic arrangement of magnussonite, redefined as $Mn^{2+}_{18}[As^{3+}_6(Mn^{1+}_x)O_{18}]_2$ $[(H_2O, Cl_x), H_2O, \square]_2$, and describe details of the atomic arrangement not recognized in the earlier study.

2. Materials and Methods

The sample examined here is from Långban, Sweden, and was obtained from the prominent Swedish mineral collectors Markus and Stefan Wiklund.

2.1. Chemical Analysis

Analyses (13 points each on two grains) were done at Caltech on a JEOL 8200 electron microprobe (JEOL Ltd., Akishima, Tokyo, Japan) in WDS mode. Analytical conditions were 15 kV accelerating voltage, 20 nA beam current and 10 µm beam diameter. The results of the analyses, including standards, are given in Table 1.

Table 1. Chemical analyses of magnussonite.

Oxide	Wt.%	Range	Standard
MnO	47.59	47.21–48.03	Mn_2SiO_4
FeO	2.1	1.97–2.29	fayalite
CaO	0.59	0.34–0.70	anorthite
CuO	0.69	0.51–0.91	Cu metal
As_2O_3	44.51	44.01–45.05	GaAs
Cl	0.27	0.21–0.32	sodalite
H_2O	0.73		
Total	96.48		
O = Cl	0.07		

Empirical formula: $(Mn^{2+}_{16.71}Fe^{2+}_{0.78}Ca_{0.28}Cu^{2+}_{0.23})_{\Sigma 18}[As_{12}Mn^{1+}_{1.19}O_{36}](H_2O_{0.99}Cl_{0.20})$.

The initial structural study of magnussonite [2] did not provide a chemical analysis but concluded that the Cl site is fully occupied $(Cl_{0.80}O_{0.20})$, although of the three earlier analyses listed in their work, only one showed significant Cl and this is only one-third of that required by the Cl assigned by them to the CLW site. Our structure and the subsequent analyses listed here also have significantly less Cl in the structure than that assumed by [2], but Cl is present in all analyses [14]. Assessing charge balance in the structure, the unit-cell contents of magnussonite can be divided into $Mn^{2+}_{144}As^{3+}_{96} = 576+$ charges, and $O_{288} = 576-$ charges, not including the MX and ClW sites of [2]. Thus, the contents of the MX site must balance the charge of the species at the ClW site. In [2], $Cl_{0.80}(OH)_{0.20}$ was assigned to CLW to balance the charge of Mn^{1+} at the fully occupied MX site. Chemical analysis of the crystal used here indicates 0.20 Cl apfu (atoms per formula unit) and the site occupancy of the CLW2 site is 0.28 Cl apfu (assigning its occupancy as Cl). The site occupancy of MX from the structure refinement gives 0.32 Mn apfu, sufficiently close to the assigned occupancy of CLW2 of 0.28 Cl to ensure the electroneutrality of the overall structure if H_2O is assigned to the CLW1 site. However, as we will see below, the incident

bond-valences at CLW1 and CLW2 (see below) do not support these assignments and also indicate that it is not possible for (OH) to occur in magnussonite.

2.2. Crystal Structure

A crystal fragment of magnussonite from Långban, Värmland, Sweden, was mounted on a Bruker Apex CCD diffractometer (Bruker Corporation, Billerica, MA, USA) equipped with graphite-monochromated Mo $K\alpha$ radiation. Refined cell parameters and other crystal data are listed in the deposited CIF file. Redundant data were collected for a sphere of reciprocal space, and were integrated and corrected for Lorentz-polarization factors and absorption using the Bruker program SAINTPLUS (Bruker Corporation, Billerica, MA, USA).

The atomic arrangement was solved in space group $Ia\bar{3}d$ (#230) using Direct Methods independent of the structure given in [2], although their atom nomenclature is used in this work. The veracity of cubic symmetry was confirmed by observation of optical isotropy of the Långban crystals. Refinement was done with anisotropic-displacement parameters for all atoms, and the structure ultimately refined to $R1 = 0.0119$ with an average redundancy of 63.1. All data processing and calculations were undertaken with the Bruker APEX3 package of programs. Crystal data and details of the refinement are contained in Table 2.

Table 2. Sample and crystal data for magnussonite.

Chemical Formula	$As_{24}Ca_{0.56}Cl_{0.40}Mn_{35.78}Fe_{1.56}O_{76.53}$
Formula weight	5016.00 g/mol
Wavelength	0.71073 Å
Crystal size	$0.069 \times 0.126 \times 0.148$ mm
Crystal habit	clear blue equant
Crystal system	Cubic
Space group	$Ia\bar{3}d$
Unit cell dimensions	a = 19.7144(5) Å
Volume	7662.2(6) Å^3
Z	4
Density (calculated)	4.348 g/cm^3
Absorption coefficient	16.096 mm^{-1}
F(000)	9246

Mn1–Mn4 were refined initially with freely varying occupancy factors because of the substitutions outlined in [2]; however, Mn3 and Mn4 refined to 1.000 within the third decimal place, and thus were fixed at full occupancy by Mn. In our structure refinement was a persistent small but distinct peak slightly displaced from the Wykoff site 16b at 1/8 1/8 1/8 and the ClW site of [2]. To confirm the reality of this peak, we refined the magnussonite atomic arrangement of two additional crystals from the same locality, mounted in random orientations. The distinct peak appeared at the same location in each structure refinement, and the magnitude of that peak is an average of 2.10 times the second largest (residual) peak for the three crystals. We thus modelled the ClW site of [2] as two sites: ClW1 and ClW2. The ClW2 site is predominantly vacant, making modeling more difficult, and refined to non-positive-definite atom-displacement parameters in the final refinement, presumably because of the very small occupancy of that site ($O_{0.11}\square_{0.89}$) and possible residual positional disorder.

Table 3 lists the refined atom parameters, Table 4 lists selected interatomic distances and Table 5 gives the bond-valence values for selected atoms (vu; valence units) calculated with the parameters of [15]. A CIF has been deposited that contains further details of crystal data and structure refinement (in Supplementary material).

Table 3. Atom coordinates and equivalent isotropic-displacement parameters (Å^2) for magnussonite. U_{eq} is defined as one third of the trace of the orthogonalized U^{ij} tensor.

Atom	x/a	y/b	z/c	U_{eq}	Site Occupancy *
Mn1	1/4	3/8	0	0.01896(12)	0.978(2) Mn^{2+} + 0.022□
Mn2	0.24001(3)	1/8	0.00999(3)	0.0248(3)	Mn^{2+}
Mn3	3/8	0.26471(2)	0.01471(2)	0.01321(5)	Mn^{2+}
Mn4	0.11269(2)	0.36269(2)	1/8	0.01017(5)	Mn^{2+}
MX	0	0	0	0.064(3)	0.158(4) Mn^{+}
As1	0.49807(2)	0.36712(2)	0.00876(2)	0.01011(4)	As^{3+}
O1	0.57129(5)	0.32307(5)	0.03197(6)	0.0265(2)	O
O2	0.46018(4)	0.31670(4)	0.94432(4)	0.01614(16)	O
O3	0.44552(4)	0.33185(5)	0.07344(5)	0.01847(17)	O
CLW1	0.0918(4)	0.1582(4)	1/8	0.029(2)	0.264(10) H_2O
CLW2	0.1175(8)	0.1325(8)	1/8	0.070(15)	0.047(4) Cl

* assigned from the refined site-scattering values and stereochemical arguments (see text).

Table 4. Selected interatomic distances (Å) in magnussonite.

Mn1-O1	2.723(1) ×4	Mn3-O1	2.057(1) ×2
Mn1-O3	2.189(1) ×4	Mn3-O2	2.407(1) ×2
<Mn1-O>	2.367	Mn3-O3	2.242(1) ×2
		<Mn3-O>	2.235
Mn2-O2	2.020(1) ×2		
Mn2-O2′	2.121(1) ×2	Mn4-O1	2.297(1) ×2
Mn2-CLW1	2.281(12)	Mn4-O2	2.180(1) ×2
Mn2-CLW1′	2.838(12)	Mn4-O3	2.171(1) ×2
Mn2-CLW2	3.10(2)	<Mn4-O>	2.216
Mn2-Mn2′	0.557(2)		
		As1-O1	1.746(1)
MX-As1	2.6256(1) ×6	As1-O2	1.778(1)
		As1-O3	1.784(1)
CLW1-CLW1	1.60(2) ×2	<As1-O>	1.769
CLW1-CLW2	0.72(2)	As1-MX	2.6257 (1)
CLW1-CLW2	1.05(2) ×2		
CLW1-Mn2	2.28(1)	CLW2-CLW2	0.36(4) ×2
CLW1-Mn2	2.84(1)	CLW2-CLW1	0.72(2)
CLW1-O2	2.974(9) ×2	CLW2-CLW1	1.05(2) ×2
		CLW2-Mn2	3.00(2)
		CLW2-Mn2	3.32(1) ×2

Table 5. Selected bond-valences * (*vu*) in magnussonite.

	As	Mn1	Mn2	Mn3	Mn4	Σ
O1	1.07	$0.10^{\times 4\downarrow}$		$0.47^{\times 2\downarrow}$	$0.26^{\times 2\downarrow}$	1.90
O2	0.98		$0.51^{\times 2\downarrow \times 0.5 \rightarrow}$ $0.40^{\times 2\downarrow \times 0.5 \rightarrow}$	$0.20^{\times 2\downarrow}$	$0.35^{\times 2\downarrow}$	1.99
O3	0.99	$0.34^{\times 4\downarrow}$		$0.30^{\times 2\downarrow}$	$0.36^{\times 2\downarrow}$	1.99
ClW1			0.27 0.07^{Ox} 0.15^{Cl}			0.27
CLW2			0.07^{Cl}			
sum	3.04	1.76	1.82 + X	1.94	1.94	

* The Mn2 site is half-occupied and positionally disordered, the bond-valence sum for O2 is written as the sum of the incident bond-valence from O2 (1.82 vu) and an unspecified amount from the possible bond-valences listed for ClW1 and ClW2.

3. Results

3.1. Site Occupancies and Coordinations

There is significant disorder at some of the sites in magnussonite and it is helpful to deal with the ordered sites first.

3.1.1. Mn1

The unconstrained occupancy for the Mn1 site refined to a value of 0.898(2) Mn, indicating another scattering species at Mn1 with an atomic number less than 25 (Mn). Vacancy is not a possibility as it would cause major deviations from the valence-sum rule (Brown 2016), leaving Ca as the only substituent (Table 1). Thus, we assign Ca to Mn1 to give an occupancy of 0.890 Mn + 0.110 Ca. The Mn1 site is surrounded by eight O^{2-} anions arranged at the corners of a distorted cube (Figure 1), with Mn1-O distances of 2.189 Å x 4 and 2.723 Å x 4, and a $<^{[8]}$Mn1-O> distance of 2.456 Å. The following ranges and mean values for $^{[4]}Mn^{2+}$-O^{2-} and $^{[8]}Mn^{2+}$-O^{2-} distances in inorganic structures are listed in [16]: $1.953 \le ^{[4]}Mn^{2+}$-$O^{2-} \le 2.194$ Å, $2.001 \le <^{[4]}Mn^{2+}$-$O^{2-}> \le 2.085$, grand $<^{[4]}Mn^{2+}$-$O^{2-}> = 2.066$ Å; $2.152 \le ^{[8]}Mn^{2+}$-$O^{2-} \le 2.691$ Å, $2.275 \le <^{[8]}Mn^{2+}$-$O^{2-}> \le 2.356$ Å, grand $<^{[8]}Mn^{2+}$-$O^{2-}> = 2.327$ Å.
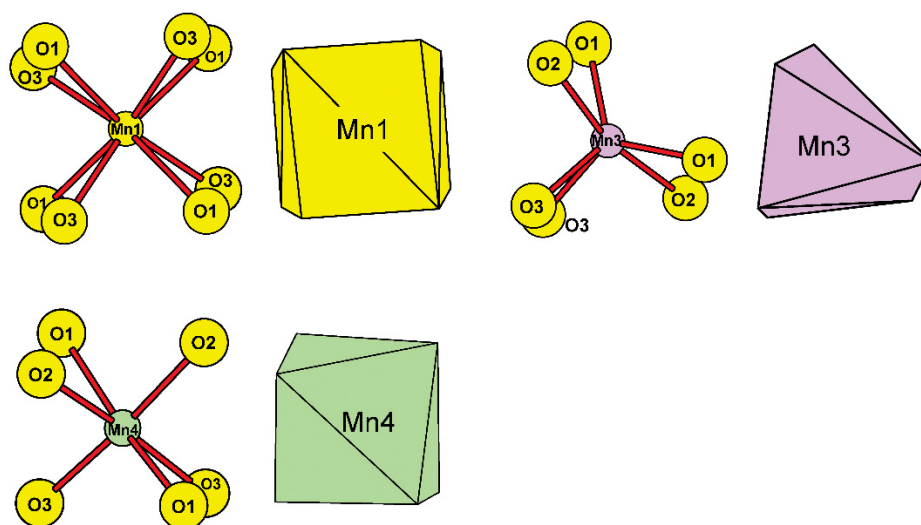

Figure 1. Coordination of Mn1, Mn3 and Mn4 polyhedra.

The longer distances in the Mn1 polyhedron lie outside these ranges both for individual bonds and for mean bond-length. The incident bond-valences at Mn1 for [4]- and [8]-coordination of Mn^{2+} are 1.36 and 1.74 *vu*, respectively, which indicates that the coordination number must be [8], despite the extreme length of the longer bonds and the deficiency in the incident bond-valence sum at the central Mn1 cation(s). The value of U^{eq} at the Mn1 site is 0.0193(1), significantly larger than the U^{eq} values at Mn3 and Mn4, suggesting that the cation may be displaced (statically or dynamically) from the central position more than is the case for the Mn3 and Mn4 cations, in accord with the anomalously long bond-lengths (Table 4) and the low bond-valence sum (Table 5). This displacement (static or dynamic) will tend to compensate for the low incident bond-valence at the central cation.

3.1.2. Mn3

The Mn3 site is coordinated by six O^{2-} anions arranged at the corners of a distorted trigonal prism (Figure 1) with Mn3–O distances in the range 2.189–2.723 Å and a <Mn1-O> distance of 2.456 Å (Table 4), and is fully occupied by Mn^{2+} (Table 3). The following range and mean value for $^{[6]}Mn^{2+}$-O^{2-} distances observed in inorganic structures are listed in [16]: $1.968 \le ^{[6]}Mn^{2+}$-$O^{2-} \le 2.798$ Å, $2.134 \le <^{[6]}Mn^{2+}$-$O^{2-}> \le 2.305$, grand $<^{[6]}Mn^{2+}$-$O^{2-}> = 2.199$ Å. All observed distances lie within these ranges both for individual bonds and for mean bond length, and the incident bond-valence sum at Mn3 is 1.940 vu (Table 5) in accord with the valence-sum rule [17].

3.1.3. Mn4

The Mn4 site is occupied by Mn^{2+} (Table 3) and is coordinated by six O^{2-} anions arranged at the corners of a distorted octahedron (Figure 1) with Mn4-O distances in the range 2.172–2.297 Å and a <Mn4-O> distance of 2.216 Å (Table 4), in accord with the observed ranges of Mn^{2+}-O^{2-} bond lengths in inorganic structures given above. Moreover, the incident bond-valence sum at Mn4 is 1.932 vu (Table 5) in accord with the valence-sum rule.

3.1.4. CLW1 and CLW2

Each of these sites is only partly occupied and the close approaches listed in Table 4 indicate that there must be extensive local order to avoid the impossible interatomic distances that are present in the long-range refinement of the structure. However, before we consider this issue, we need to return to the long-range occupancies of these sites. Inspection of Table 4 shows that the only Mn–CLW1 distances that can be considered as bonds are 2.28 and 2.84 Å. CLW1 is potentially occupied by O, (OH), (H_2O) and/or Cl. The relevant interatomic distances and corresponding bond-valences for these species at CLW1 are as follows: O, (OH) and (H_2O): 2.28 Å: 0.27 vu; 2.84 Å: 0.07 vu; Cl: 2.28 Å: 0.67 vu; 2.84 Å: 0.15 vu. It is immediately apparent that of the O-bearing species, only (H_2O) can occur at CLW1; the occurrence of O and (OH) at CLW1 strongly violates the valence-sum rule. For Cl, the incident bond-valence at CLW1 for the distance 2.84 Å is not in accord with the valence-sum rule; the incident bond-valence of 0.67 vu at CLW1 for the distance 2.28 Å is rather more ambiguous as it is much closer to the ideal value of 1 vu, but the distance is much shorter than Mn–Cl distances observed in inorganic structures.

Table 4 shows that the CLW2 site is close only to the Mn2 site which is completely occupied by Mn^{2+} with a Mn2-CLW2 distance of 3.00 A and corresponding incident bond-valences for [O, (OH) and (H_2O)] and Cl of 0.05 and 0.10 vu, respectively. Neither of these values allows O, (OH) or Cl to occur at the CLW2 site, whereas the very low value of 0.05 vu allows (H_2O) to occur at CLW2.

These arguments provide somewhat of a conundrum. On the one hand, bond-valence considerations seem to discount the possibility that there are ions (as distinct from neutral species) at the CLW1 and CLW2 sites (except for the possibility of a small amount of Cl at CLW1). On the other hand, (1) the $(Mn^{2+} + M^{2+})_{18}$ [$As_{12}O_{36}$] part of the structure is electroneutral and the content of the CLW1 and CLW2 sites must balance the charge of the cation(s) at the MX site, and (2) several chemical analyses of magnussonite show significant Cl [14]. We will attempt to locate a crystal of magnussonite with a much higher content of Cl in order to further understand the charge-balance mechanism(s) associated with the channel species in magnussonite.

3.1.5. Mn2

The Mn2 atom is slightly displaced from the 24c site at 1/4 1/8 0 to occupy the 48 g site at x 1/8 z; the ensuing Mn2-Mn2 distance is 0.557 Å, and only one of these two sites can be locally occupied. The aggregate Mn2 site is occupied by 1.0 Mn^{2+} and is surrounded by six anion sites: four O2 sites, fully occupied by O^{2-} and with Mn2-O distances of 2.020×2 Å and 2.121×2 Å, and two CLW1 sites, partly occupied by (H_2O) (and possibly minor Cl) and with Mn2-CLW1 distances of 2.281 Å and 2.838 Å. The actual coordination of the cation occupying the Mn2 site is somewhat more complicated as (1) the presence of two split sites gives a set of interatomic distances not all of which are adopted in the local (short-range) arrangements in the structure; (2) the split sites are forced by the $Ia\bar{3}d$ symmetry of the overall structure to be equally occupied, and this is not necessarily the case as the local symmetry cannot accord with $Ia\bar{3}d$ as this would result in fractional atoms at these sites.

The Mn2 cation has four O2 anions forming a quadrilateral with both of the split sites approximately at its center, with an incident bond-valence of 1.824 vu at each of the central cations (Table 5). In addition, there are atoms at the CLW1 site(s) that provide additional

coordination. In terms of the Mn2 cations with a collective occupancy of 1.0, there are $1.58/3 = 0.53$ (H_2O) groups (and possibly minor Cl) at CLW1. The long-range chemical formula of Mn2 and its coordinating anions is $Mn\varphi_{4.5}$, $\varphi = O^{2-}$, (H_2O), and Occam's razor suggests that we may write this as follows: $Mn\varphi_{4.5} = 0.5\ MnO_4 + 0.5\ MnO_4(H_2O)$. Thus, Mn2 has two local coordinations: $Mn2O_4$ and $Mn2O_4(H_2O)$. $Mn2O_4$ has a coordination intermediate between tetrahedral and square planar (Figure 2a), resembling a flattened tetrahedron. $Mn2O_4(H_2O)$ forms a square pyramid with (H_2O) at the apex of the polyhedron (Figure 2a).
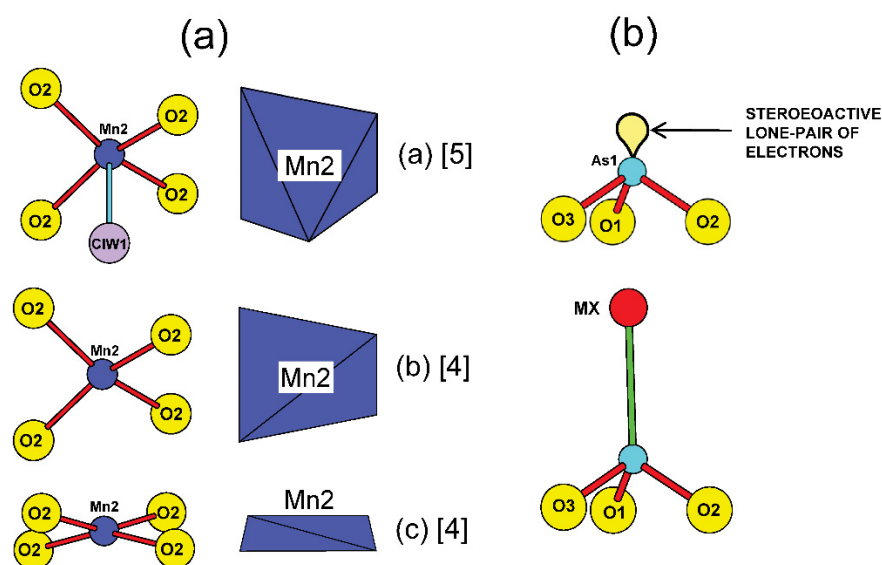
Figure 2. (**a**) Local coordinations of Mn2 (explanation in text). (**b**) Coordination of As atom, depicting lone-pair electrons and coordination to MX in partly occupied site.

The Mn2CLW1 distances of 2.28 and 2.84 result in bond valences of 0.27 and 0.07 vu, respectively, if CLW1 is occupied by (H_2O) as discussed above. This gives incident bond-valence sums of 2.09 and 1.89 vu, both of which are in reasonable accord with the valence-sum rule. Where in tetrahedral coordination, the incident bond-valence sum at Mn2 is 1.82 vu; this is somewhat low with regard to the valence-sum rule, but U^{eq} at the Mn2 site is 0.0249(1), significantly larger than the U^{eq} values at Mn3 and Mn4, as is often the case where the incident bond-valence falls significantly below its ideal value. What is not clear is whether the long-range orientation of the square pyramid is ordered or disordered; refining the structure in *Ia3d* symmetry forces the square pyramid to be long-range orientationally disordered, but there is insufficient scattering associated with orientational order to enable this issue to be decided by refinement in lower symmetry.

3.1.6. As1

The As1 site is fully occupied by As^{3+} that is bonded to three O^{2-} ions in the trigonal pyramidal arrangement (Figure 2b) that is typical for lone-pair-stereoactive As^{3+}, with a <As-O> distance of 1.769 Å (Table 4), close to the grand mean value of 1.776 Å given in [18] for <As^{3+}-O_3> in inorganic structures. Commonly, As^{3+} in ($As^{3+}O_3$) is lone-pair stereoactive and the lone pair of electrons projects out from the cation on the side opposing the three O^{2-} ions (Figure 2b). However, the partly occupied MX site occurs 2.626 Å from As^{3+} and its constituent cation must be considered as bonding to As^{3+} (Figure 2b).

3.1.7. MX

The MX site is occupied by ($Mn_{0.158(4)}\square_{0.842}$) and is surrounded by six As^{3+} ions arranged at the corners of an octahedron, with six equal MX-As distances of 2.6256(1) Å (Table 4). Figure 3 shows this site and its coordinating ions viewed down [111]. This atomic arrangement is unique and the bonding of a third-row transition metal to As^{3+}

is rare; only dixenite [13] and the synthetic compounds $Cu(tclH)_2(AsPh_3)Br$ [19] and $Cu(tclH)(AsPh_3)_2Br$ [20] show Cu^+–As^{3+} bonds.
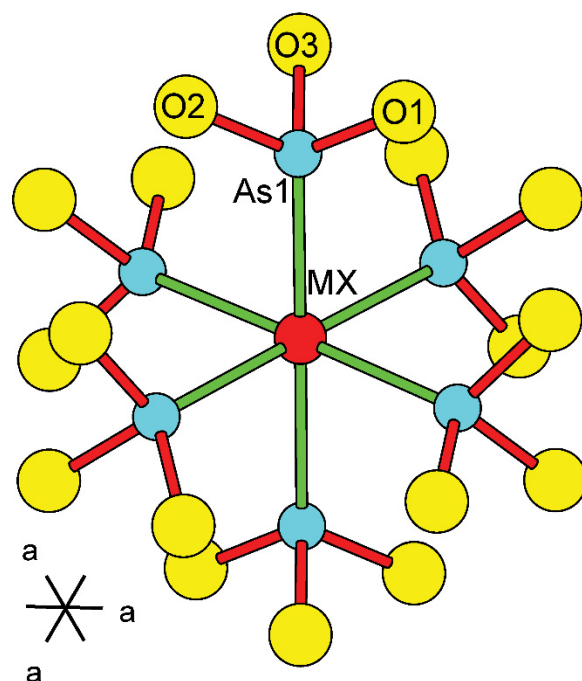

Figure 3. Coordination of channel MX site in magnussonite.

4. Bond Topology

Magnussonite has a densely packed structure of $(Mn\varphi_n)$ polyhedra, $\varphi = (O^{2-}, H_2O, Cl^-)$, and $(As^{3+}O_3)$ triangular pyramids that is best envisaged as layers of polyhedra in the same way as many other of the manganese-arsenite-arsenate structures from Långban (Figure 4). Polyhedra are referred to by their central site: thus $(Mn1O_8)$ is the Mn1 polyhedron or cube. There are two distinct layers in magnussonite, designated layer A and layer B in Figure 4. The two layers may be combined into a slab, AB, that stacks along the **a**-direction with rotations between adjacent slabs (Figure 4). Each layer is shown in Figure 5, both in cross-section and in plan. Layer A (Figure 5a) consists of a complicated array of edge-sharing $(Mn\varphi_n)$ polyhedra. A prominent two-dimensional motif involves four Mn4 octahedra (pale green) arranged at the corners of a square and sharing edges with an Mn1 cube (yellow) at the centre of the square. These square clusters link to each other by sharing edges with Mn3 trigonal prisms (lilac) that are surrounded by three Mn4 octahedra to form an open network with large spaces that are braced by Mn2 polyhedra (dark blue, shown as square-planar arrangements in Figure 5a). As is apparent in the edge-on view, the surface of layer A is decorated by As1 triangular pyramids. Layer B (Figure 5b) consists of a square latticework of Mn1 (yellow), Mn2 (dark blue) and Mn3 (lilac) polyhedra linked by As1 triangular pyramids. The Mn1 cube shares edges with the Mn3 trigonal prism and the Mn2 polyhedron shares corners with the Mn3 trigonal prism, and the four-membered clusters (in plan view) are linked into a sheet by sharing corners with As1 triangular pyramids. Again, as is apparent in the edge-on view (Figure 5b), the surface of layer A is decorated by As1 triangular pyramids. Comparison of the edge views in Figure 5 with the view of the complete structure in Figure 4 shows that the As1 triangular pyramids nominally assigned to one layer in Figure 5 actually penetrate the other layer, resulting in a hard and brittle structure.
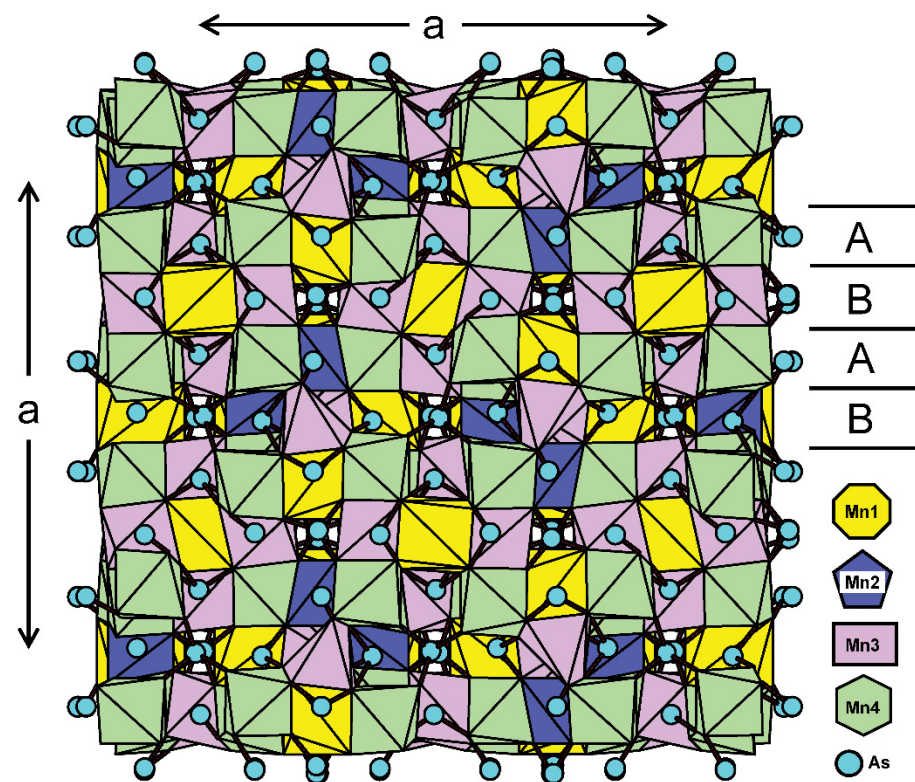
**Figure 4.** Stacking of A and B layers in magnussonite.
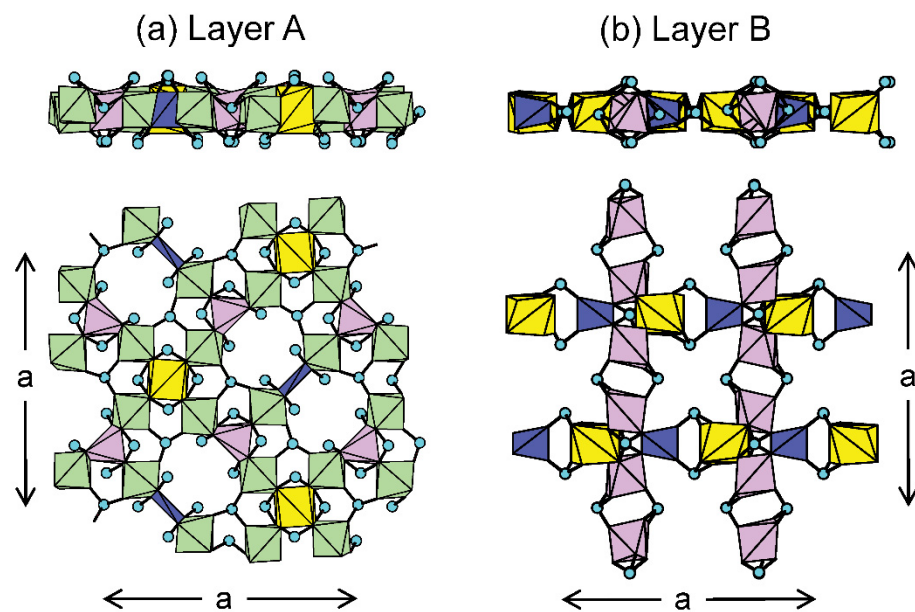
Figure 5. Depiction of individual (**a**) A and (**b**) B layers in magnussonite, in cross-section (**upper**) and in plan view (**lower**).

Viewing the structure down [111], an array of channels becomes apparent (Figure 6), a surprising feature in such a dense-packed structure. These channels contain much of the disorder that occurs in the magnussonite structure. The partly occupied MX site occurs at the Wykoff site 16a on the central axis of the channel, and the CLW2 site (with extremely low occupancy) occurs at the off-axis 48g site, slightly disordered off the Wykoff site 16b, also on the central axis of the channel.
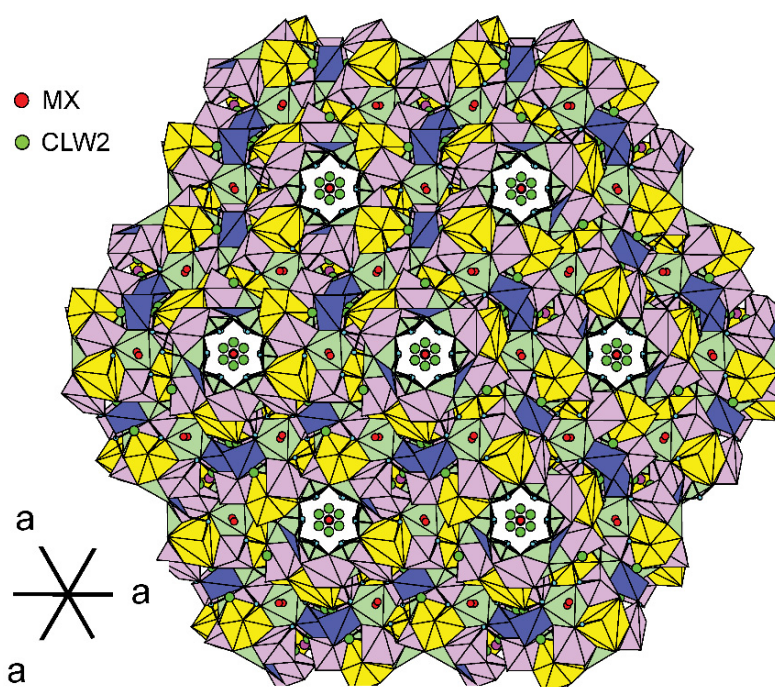
Figure 6. View of magnussonite atomic arrangement down [111], illustrating the channels in structure.

The [Mn⁺(As³⁺O₃)₆] Arrangement

The structure solution and refinement of [2] reported full occupancy of the MX site that was also displaced from the Wykoff position 16a at 0 0 0 by 0.30 Å, resulting in a range of MX-As1 distances; however, we found no evidence of such disorder in our crystal with a partly occupied MX site.

The partly occupied MX site occurs on the central axis of the continuous channels through the structure (Figure 6), and the question arises as to how such an irregularly shaped entity as that shown in Figure 3 can fit into such a densely packed structure. The local arrangement around the unoccupied MX site is shown in Figure 7a. The $(As^{3+}O_3)$ groups attach to different layers of Mn3 trigonal prisms and Mn4 octahedra outward from the central axis of the channel and the associated stereoactive lone-pairs of electrons project into the channel (Figure 7a). Where the MX site is occupied by Mn, there are six lone-pairs of electrons pointing toward Mn; what happens? The 18-electron rule predicts/rationalizes formulae for stable transition-metal clusters. The valence orbitals in the third-row transition metals consist of five 3*d* orbitals, one 3*s* orbital and three 3*p* orbitals that can collectively accommodate 18 electrons as either bonding or nonbonding electron pairs, filling the outer shell. In [2], the $[Mn^+(As^{3+}O_3)_6]$ arrangement was interpreted as forming in accord with the 18-electron rule where Mn^+ contributes 6 3*d* electrons and the six lone-pairs of the $[(As^{3+}O_3)_6]$ arrangement (Figure 7a) contribute 12 electrons for a total of 18 electrons that form nine molecular orbitals that are metal-ligand bonds (Figure 7b) or non-bonding. This scheme is also in accord with the $[Cu^+(As^{3+}O_3)_4]$ arrangement in dixenite [1,13] in which Cu^+ contributes 10 electrons and the four lone-pairs of the $[(As^{3+}O_3)_4]$ arrangement contribute 8 electrons for a total of 18 electrons. However, the reason why these $[M^+(As^{3+}O_3)_n]$ clusters form in these two minerals and are completely unknown in any other mineral or synthetic inorganic structure is still obscure. It should also be noted that the occurrence of Mn^+ and Cu^+ in these structures is deduced via the 18-electron rule, and direct confirmation of their unusual oxidation state is desirable.
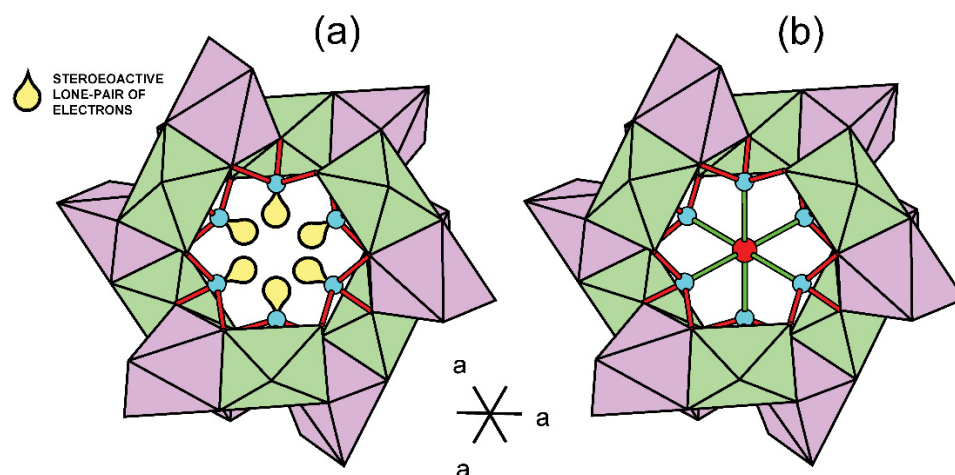
Figure 7. Local arrangement around (**a**) unoccupied MX site, and (**b**) occupied MX site in magnussonite channels.

5. Discussion

The basic manganese-iron arsenate-arsenite-silicate minerals of the Långban-type deposits in Bergslagen, Sweden, form a family of very complicated layer structures, several of which contain local exotic atomic arrangements embedded within their close-packed structures. Examples are the $[Cu^+(As^{3+}O_3)_4]$ cluster in dixenite and the $[Mn^{2+}_3O_{12}]$ cluster in magnussonite, and the local replacement of an $(As^{3+}O_3)$ group by a $(Mg, Mn^{2+}_3O_{13})$ cluster in mcgovernite and carlfrancisite [9]. The presence of these exotic clusters in structures containing densely packed Mn^{2+} octahedra is not understood at the moment. With only two minerals containing such metal clusters in an oxide matrix, combined with their low abundance in each structure, little is known about them as yet.

References

1. Araki, T.; Moore, P.B. Dixenite, $Cu^{1+}Mn_{14}^{2+}Fe^{3+}(OH)_6(As^{3+}O_3)_5(As^{5+}O_4)$: Metallic $[As_4^{3+}Cu^{1+}]$ clusters in an oxide matrix. *Am. Mineral.* **1981**, *66*, 1263–1273.
2. Moore, P.B.; Araki, T. Magnussonite, manganese arsenite, a fluorite derivative structure. *Am. Mineral.* **1979**, *64*, 390–401.
3. Gabrielson, O. Magnussonite, a new arsenite mineral from the Långban Mine in Sweden. *Ark. Mineral. Och. Geol.* **1956**, *2*, 133–135.
4. Moore, P.B. Mineralogy and chemistry of Långban type deposits in Bergslagen, Sweden. *Mineral. Rec.* **1970**, *1*, 154–172.
5. Holtstam, D.; Langhof, J. (Eds.) *Långban: The Mines, Their Minerals, Geology and Explorers*; Raster Förlag: Stockholm, Sweden, 1999; p. 215.
6. Lundström, I. General Geology of the Bergslagen Ore Region. In *Långban: The Mines, Their Minerals, Geology and Explorers*; Holtstam, D., Langhof, J., Eds.; Raster Förlag: Stockholm, Sweden, 1999; pp. 19–27.

7.　Bollmark, B. Some Aspects of the Origin of the Deposit. In *Långban: The Mines, Their Minerals, Geology and Explorers*; Holtstam, D., Langhof, J., Eds.; Raster Förlag: Stockholm, Sweden, 1999; pp. 43–49.

8.　Nysten, P.; Holtstam, D.; Jonsson, E. The Långban Minerals. In *Långban: The Mines, Their Minerals, Geology and Explorers*; Holtstam, D., Langhof, J., Eds.; Raster Förlag: Stockholm, Sweden, 1999; pp. 89–183.

9.　Hawthorne, F.C. Long-range and short-range cation order in the crystal structures of Carlfrancisite and Mcgovernite. *Mineral. Mag.* **2018**, *82*, 1101–1118.

10.　Hawthorne, F.C.; Abdu, Y.A.; Ball, N.A.; Pinch, W.W. Carlfrancisite: $Mn^{2+}_3 (Mn^{2+},Mg,Fe^{3+},Al)_{42}[As^{3+}O_3]_2(As^{5+}O_4)_4[(Si,As^{5+})O_4]_6 [(As^{5+},Si)O_4]_2(OH)_{42}$, a new arseno-silicate mineral from the Kombat mine, Otavi valley, Namibia. *Am. Mineral.* **2013**, *98*, 1693–1696. [CrossRef]

11.　Cooper, M.A.; Hawthorne, F.C. The effect of differences in coordination on ordering of polyvalent cations in close-packed structures: The crystal structure of arakiite and comparison with hematolite. *Can. Mineral.* **1999**, *37*, 1471–1482.

12.　Cooper, M.A.; Hawthorne, F.C. The crystal structure of kraisslite, $^{[4]}Zn_3(Mn,Mg)_{25}(Fe^{3+},Al)(As^{3+}O_3)_2[(Si,As^{5+})O_4]_{10}(OH)_{16}$, from the Sterling Hill mine, Ogdensburg, Sussex County, New Jersey, USA. *Mineral. Mag.* **2012**, *76*, 2819–2836. [CrossRef]

13.　Hawthorne, F.C.; Hughes, J.M. The suppression of lone-pair-stereoactivity in $[Cu^+(As^{3+}O_3)_4]$ clusters in dixenite: A tribute to Paul B. Moore. *Am. Mineral.* **2021**, *106*, 1580–1585. [CrossRef]

14.　Dunn, P.J.; Ramik, R.A. Magnussonite: New chemical data, an occurrence at Sterling Hill, New Jersey, and new data on a related phase from the Brattfors mine, Sweden. *Am. Mineral.* **1984**, *69*, 800–802.

15.　Gagné, O.C.; Hawthorne, F.C. Comprehensive derivation of bond-valence parameters for ion pairs involving oxygen. *Acta Crystallogr.* **2015**, *B71*, 562–578. [CrossRef] [PubMed]

16.　Gagné, O.C.; Hawthorne, F.C. Bond-length distributions for ions bonded to oxygen: Results for the transition metals and quantification of the factors underlying polyhedral distortion via bond-length variation. *IUCrJ* **2020**, *7*, 581–629. [CrossRef]

17.　Brown, I.D. *The Chemical Bond in Inorganic Chemistry. The Bond Valence Model*, 2nd ed.; Oxford University Press: Oxford, UK, 2016.

18.　Gagné, O.C.; Hawthorne, F.C. Bond-length distributions for ions bonded to oxygen: Metalloids and post-transition metals. *Acta Crystallogr.* **2018**, *B74*, 63–78. [CrossRef]

19.　Karagiannidis, P.; Akrivos, P.D.; Mentzafos, D.; Terzis, A. New class of Cu(I) complexes with 2-thioxohexamethyleneimine (tclH) and Group VA donors. Crystal structure of $[Cu(tclH)_2(AsPh_3)Br]$. *Inorg. Chim. Acta* **1991**, *181*, 263–267. [CrossRef]

20.　Karagiannidis, P.; Akrivos, P.; Aubry, A.; Skoulika, S. Synthesis and study of mixed ligand monomer Cu(I) compounds with Cu-As bonds. Crystal and molecular structure of bis(triphenylarsine)-(2-thioxohexamethyleneimine) copper(I) bromide. *Inorg. Chim. Acta* **1991**, *188*, 79–83. [CrossRef]